Journal of Mechanical Engineering and Sciences (JMES)
ISSN (Print): 2289-4659; e-ISSN: 2231-8380; Volume 5, pp. 713-722, December 2013

DOI: http://dx.doi.org/10.15282/jmes.5.2013.18.0069

TRANSIENT SEMI-CIRCULAR LID-DRIVEN CAVITY FLOW USING NON-UNIFORM STRUCTURED GRID METHOD WITH UPWIND SCHEME

M.S. Idris[1*], N.M.M. Ammar[1], T.M.Y.S. Tuan Ya[1] and A. M. Amin[1]

[1]Faculty of Mechanical Engineering, Universiti Malaysia Pahang (Energy Information Bureau (EIB) Malaysia),
26600 Pekan, Pahang, Malaysia
*Email: idriss@ump.edu.my
Phone: +609-424-6233; Fax: +609-424-2202
Email: idriss@ump.edu.my

ABSTRACT

In this article, two-dimensional lid-driven cavity flow in a semi-circular cavity is simulated using a non-uniform finite different method with structured grid. Navier-Stokes and continuity equations are simplified using a non-dimensional streamfunction–vorticity approach. A Reynolds number of 1000 is used and the vorticity and streamfunction contour plot is monitored with convergence criteria of $1x10^{-7}$ set to both the vorticity and the streamfunction value. The result shows that the primary vortex moves from the upper left cavity corner to the upper right corner, while the magnitude of the streamfunction grows at the primary vortex center. The primary vortex size decreases steadily as the time increases. This phenomenon is greatly affected by the increasing size of the secondary vortex at the lower left. Slight changes of vortex size are observed as the flow achieves a steady state condition. Validation of the simulation results shows the current value deviation from the established result is less than 5%. In future, it is recommended to use a better numerical method so that the simulation is more stable and so that the calculation time can be reduced.

***Keywords*:** Cavity flow; finite difference method; semi-circular; non-uniform grid.

INTRODUCTION

There are many applications of lid-driven cavity flow considering the fluid-particle interaction which is available in industrial applications including fluidized beds, pneumatic or slurry transport of dusts, coal combustion, dust explosions and catalytic reactions(Kosinski, Kosinska, & Hoffmann, 2009). There are enormous numbers of articles regarding lid-driven cavity flow, one of the most cited of which is by Ghia, Ghia, and Shin (1982). Patankar (1980) has also shown great examples for simulation of lid-driven cavity flow which have been considered in hundreds of papers as their main references. There are many other research papers, most of which intend to use the lid-driven cavity problem as a test case for a new scheme(Azwadi & Idris, 2010; Barragy & Carey, 1997; Cheng & Hung, 2006; Zin & Sidik, 2010), rather than studying the behavior of the flow pattern. In lid-driven cavity flow, there are many variations of research that have been conducted and published compared to the original condition, which use two-dimensional square cavities and a driven top lid. Examples of these variations are a two-sided driven cavity (Albensoeder, Kuhlmann, & Rath, 2001) a four-sided driven cavity(Wahba, 2009), a triangular cavity(Erturk & Gokcol, 2007), a trapezium cavity(Zhang, Shi, & Chai, 2010)), convection mixed (Azwadi & Idris,

2010) and even a semi-circular cavity, which is quite recent for lid-driven cavity flow. On the semi-circular cavity, there are only a few research papers and the basic variation is the Reynolds number, which ranges from 100 to 6600. Glowinski, Guidoboni, and Pan (2006)used the finite element method, Mercan and Atalık (2009)used a skewed grid, Yang, Shi, Guo, and Sai (2012) used the lattice Boltzmann method and according to the results, found that the streamline patterns are identical even though the methods and schemes used differ. A non-uniform grid with the finite difference method has never been tested before, to the authors' knowledge after thorough research. However, while there is already a report based on this method, it is applied to an elliptical shaped lid-driven cavity flow(Idris, Ammar, & M Irwan, 2012). Thus, in this study a non-uniform grid and finite difference method will be applied to a semi-circular cavity to obtain validation, and once this is completed, the transient behavior of the streamline and vorticity contour will be studied until the steady state is achieved. The location of the primary vortex center will also be considered. The method to be used is the streamfunction– vorticity approach with a non- uniform finite difference method.

MATHEMATICAL MODEL

To obtain the simulation results, the following continuity equation and momentum equation are used in Cartesian coordinates. Cylindrical coordinates will not be applied as this would introduce complexity. Meanwhile, a non-uniform grid and special modification are used to facilitate the curvature boundary at the bottom part of the cavity. The streamfunction–vorticity approach is essential as the velocity, *U*, *V* and pressure, *P* is reduced to only two parameters, which are the streamfunction, Ψ and vorticity, Ω. These equations are then reduced to a dimensionless vorticity equation and a vorticity transport equation.

Continuity:
$$\frac{\partial u}{\partial x}+\frac{\partial v}{\partial y}=0 \tag{.1}$$

X-momentum
$$\frac{\partial u}{\partial t}+u\frac{\partial u}{\partial x}+v\frac{\partial u}{\partial y}=-\frac{\partial p}{\partial x}+\frac{\mu}{\rho}\left[\frac{\partial^2 u}{\partial x^2}+\frac{\partial^2 u}{\partial y^2}\right] \tag{2}$$

Y-momentum
$$\frac{\partial v}{\partial t}+u\frac{\partial v}{\partial x}+v\frac{\partial v}{\partial y}=-\frac{\partial P}{\partial y}+\frac{\mu}{\rho}\left[\frac{\partial^2 v}{\partial x^2}+\frac{\partial^2 v}{\partial y^2}\right] \tag{3}$$

Dimensionless vorticity transport equation

$$\frac{\partial \Omega}{\partial T}+U\frac{\partial \Omega}{\partial X}+V\frac{\partial \Omega}{\partial Y}=\frac{1}{Re}\left[\frac{\partial^2 \Omega}{\partial X^2}+\frac{\partial^2 \Omega}{\partial Y^2}\right] \tag{4}$$

Dimensionless vorticity equation in streamfunction

$$\frac{\partial^2 \Psi}{\partial X^2}+\frac{\partial^2 \Psi}{\partial Y^2}=-\Omega \tag{5}$$

The central finite difference for the spatial derivative of the non-uniform grid and a first order upwind scheme (explicit) for the temporal derivative were implemented

to provide a simulation of the transient behavior. First and second order derivatives of the non-uniform grid approximation were used and represented by the following equations (Idris et al., 2012) which were first discovered by(Veldman & Rinzema, 1992):

$$\frac{\partial f}{\partial x} \cong \frac{f(x_{i+1}) - f(x_{i-1})}{\Delta x_a + \Delta x_b} \tag{6}$$

$$\frac{\partial^2 f}{\partial x^2} \cong \frac{2f(x_{i+1})}{\Delta x_a(\Delta x_a + \Delta x_b)} - \frac{2f(x_i)}{\Delta x_a \Delta x_b} + \frac{2f(x_{i-1})}{\Delta x_b(\Delta x_a + \Delta x_b)} \tag{7}$$

and for the physical formulation, the collocated nodes of the non-uniform grid size are presented in Figure 1.

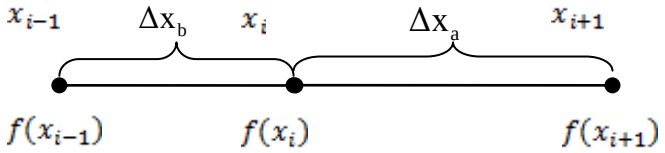

Figure 1. Non uniform grid for collocated node

The dimensionless variables are represented by the following equation:

$$U = \frac{u}{U_{Top}}, \quad V = \frac{v}{U_{Top}}, \quad \Psi = \frac{\psi}{U_{top} D}, \quad \Omega = \frac{\omega D}{U_{top}}, \tag{8}$$

$$X = \frac{X}{W}, \quad Y = \frac{D}{W}, \quad T = \frac{U_{top} t}{W}, \quad Re = \frac{\rho U_{top} W}{\mu} \tag{9}$$

GRID GENERATION

The grid used in the simulation is 100 x 50. It is difficult to convey the idea of a non-uniform grid using the original grids, so in Figure 2, 12 x 6 grids are used to express the idea of providing a semi-circular cavity. Black dots represent the boundary, white dots represent the non-calculated or cavity outer part and the dashed dots represent the internal nodes where numerical calculation takes place, or in other words, the computational domain. From the triangular cavity, it is possible to convert it into a semi-circular cavity by carefully adjusting the grid size of individual rows and columns. The grids are arranged in a manner where at the circle center the gaps are bigger and at the end of the radius, the gaps are smaller. A normal finite difference equation is not suitable for this kind of boundary, so to satisfy the boundary, non-uniform finite difference is used. The test case physical system is shown in Figure 3, where *a* is the primary vortex and *b* is the secondary vortex.

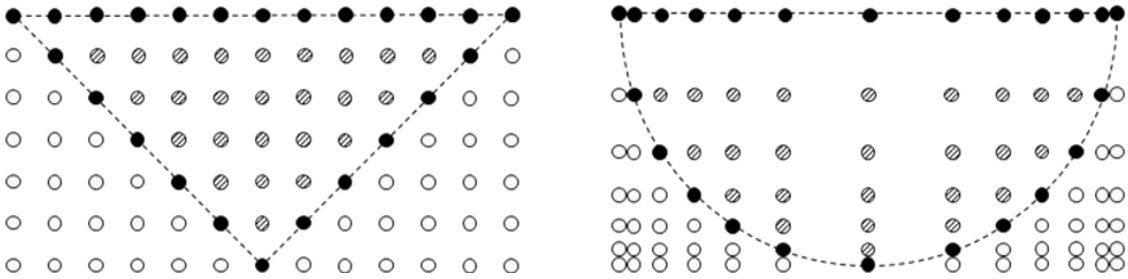

Figure 2. Grid of semi-circle

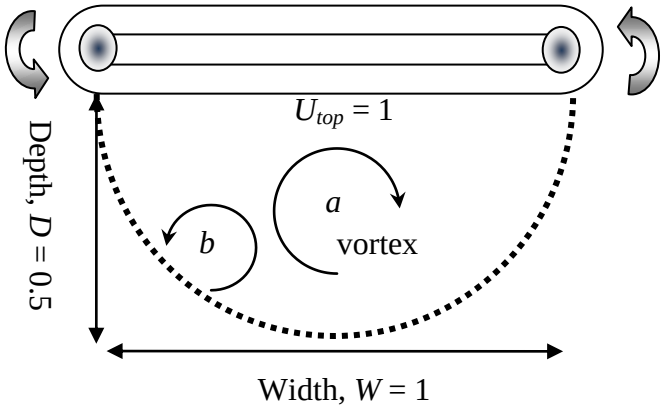

Figure 3. Semi-circular lid-driven cavity physical test case

The boundary conditions play a major role for the simulation as incorrect interpretation of the boundary condition will affect the final solution of the simulation. For the boundary condition, again, the non-uniform grid method is applied especially for the vorticity boundary condition and top lid *U* velocity.

Table 1. Boundary conditions for semicircular driven cavity flow

Boundary	U	V	Ψ	Ω
Top	1	0	0	$\frac{\partial^2\Psi}{\partial X^2}+\frac{\partial^2\Psi}{\partial Y^2}=-\Omega$
Curve	0	0	0	$\frac{\partial^2\Psi}{\partial X^2}+\frac{\partial^2\Psi}{\partial Y^2}=-\Omega$

VALIDATION

In this study, validation was conducted based on the steady state results for Reynolds number 1000 in line with (Glowinski et al., 2006) both for the highest streamfunction value and for the primary vortex center location. The previous result by Glowinski et al. (2006) is selected as the basis of percentage differences. This value is actually taken once the steady state condition is achieved. The exact time required for the center location to achieve a steady state is not available, as the research was not about the

transient condition. Thus, this comparison is solely based on the steady state condition. Further increase of residue monitoring or using smaller convergence criteria is not required as the result of using a smaller value yields similar or only tiny changes to the current simulation settings. The validation is presented in Table 2, where, according to the results, the value percentage is less than 5%, which makes it acceptable for validation purposes.

Table 2. Boundary conditions for semi-circular driven cavity flow

Result	Ψ	$\%\Delta\Psi$	X_{location}	$\%\Delta X_{\text{loc.}}$	Y_{location}	$\%\Delta Y_{\text{loc.}}$
(Glowinski et al., 2006)	-0.07800		0.6156		-0.2042	
Present	-0.07586	2.7%	0.6243	1.4%	-0.1986	2.7%

RESULTS AND DISCUSSION

In this section, there will be a discussion regarding the location of the vortex center and the total time required to achieve the center location. According to previous experimental research, it takes 27.55 seconds or dimensionless time, t^* 8 to achieve a steady state(Migeon, Texier, & Pineau, 2000). This result is parallel to the current findings that the final stage or time to reach a steady state is 27.7 seconds. However, the previous results did not show a secondary vortex, due to different conditions, since the previous result was based on 3D settings. Another reason supporting this is that the streamfunction value of the secondary vortex is too small compared to the primary vortex and it existence cannot be captured on camera. For a Reynolds number of 1000, to achieve the steady state condition, more than 5 million iterations are required, which takes about 24 hours using an Intel Xeon processor, with two out of twelve cores operating. However, in real application, it requires only about 25 seconds, where the dimensionless time increment is only 5×10^{-6}. The small value of time increment is used to prevent an error-prone condition, as advised by Courant–Friedrich–Lewy, especially for explicit numerical methods. Only a few results out of the 5 million iterations are plotted and shown in Figure 4, which is the transient behavior of the streamline pattern. For both Figures 5 and 6, (a) is 0.000415 seconds, (b) is 0.18728 seconds, (c) is 0.78081 seconds, (d) 1.257 seconds, (e) 2.566 seconds, (f) is 5.239 seconds, (g) is 6.14 seconds, (h) is 7.2 seconds, (i) is 8.433 seconds and (j) is 27.7 seconds. At first, the vortex center is not visible and as the time increases by about one second, the primary vortex center appears at the top right corner of the cavity. The primary vortex center then moves slowly to the bottom and left section of the cavity and the intensity of the streamfunction increases. As the time reaches 5 seconds, signs of a secondary vortex are appearing and it finally shows itself at around 6 seconds of physical time. The secondary vortex steadily grows and occupies some of the primary vortex area at the lower left bottom. When the time approaches 25 seconds, the size of the secondary vortex gradually increases. As a consequence, the primary vortex decreases in size.

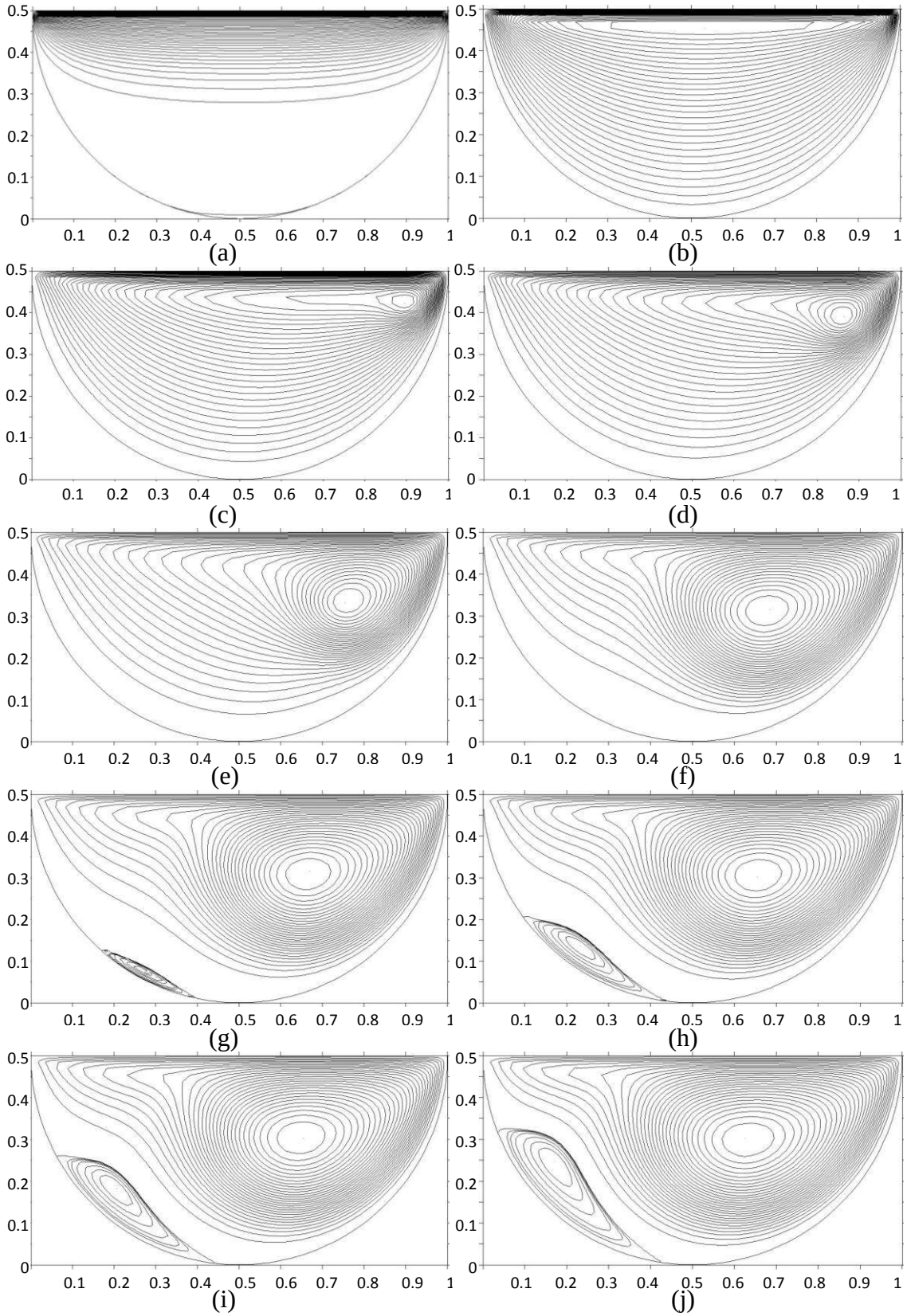

Figure 4. Transition streamlines pattern for semi-circular cavity flow for Reynolds number 1000 from (a) to (j)

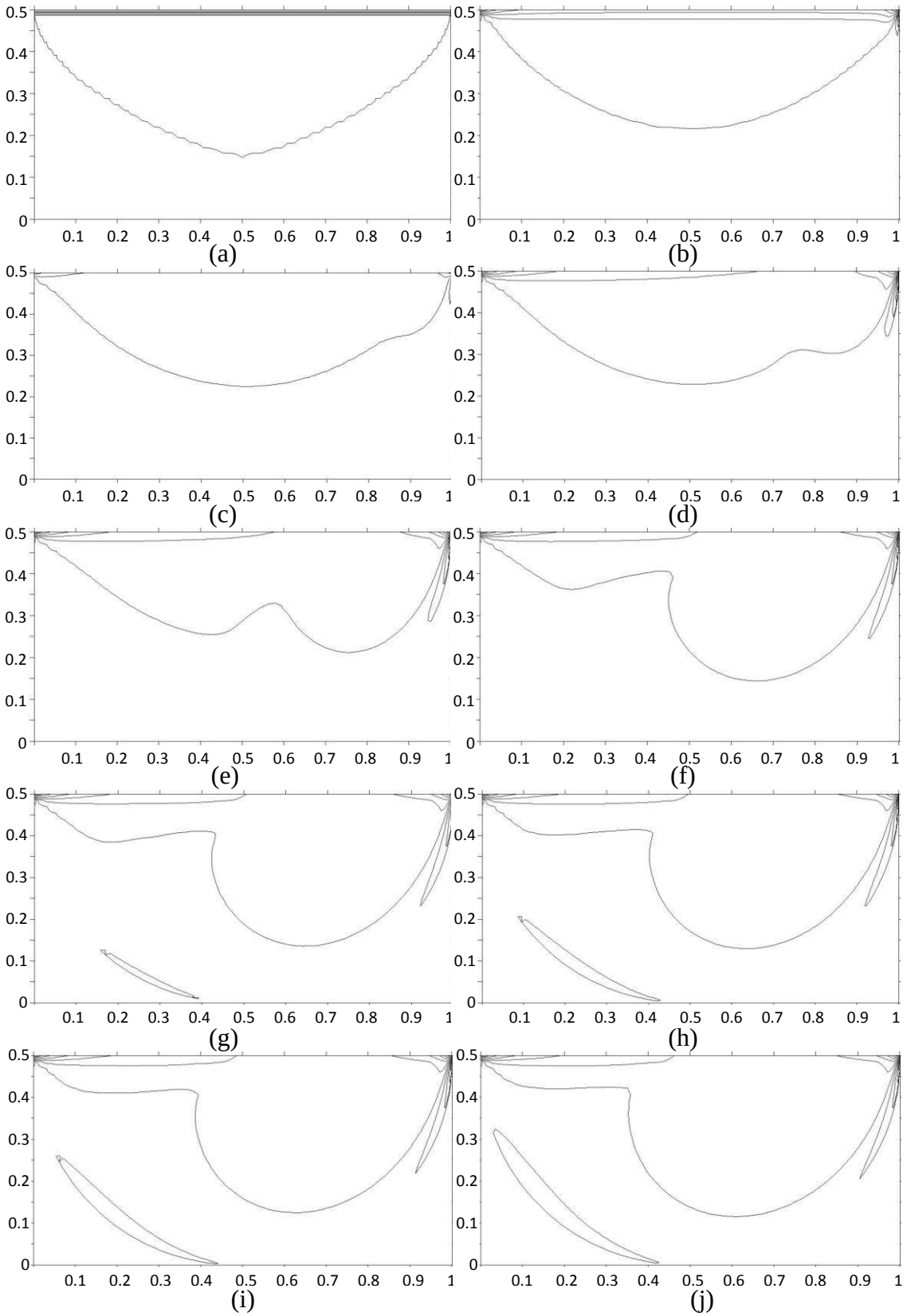

Figure 5. Transient vorticity contour for semi-circular cavity flow for Reynolds number 1000 from (a) to (j)

Meanwhile for the vorticity contours shown in Figure 6, rapid changes of pattern appear for physical times between 1 to 8 seconds. It is impossible to plot the center of the primary vortex for each iteration ranging from 1 to 5000000 iterations, so just a few selected results are plotted and shown in Figure 6. The *X*-axis represents the width of the cavity and *Y*-axis represents the height of the cavity. The position of the primary vortex center actually moves from the middle top section and towards the right cavity section. This condition only happens for a physical time of around 1 second. As the time increases, the point moves downward and towards the middle section, until it settles at 27.7 seconds at location (0.6243, 0.3014) when the simulation has achieved the steady state, which is compared to previous experimental results. This is because the primary vortex's streamfunction values start from the top level and slowly transfer the magnitude to the lower section. During the earlier period, the streamfunction value is zero at the bottom, so the center location is near to the top level. As the simulation achieves a steady state, there are streamfunction values at the bottom section which cause the center location to move lower toward the bottom.

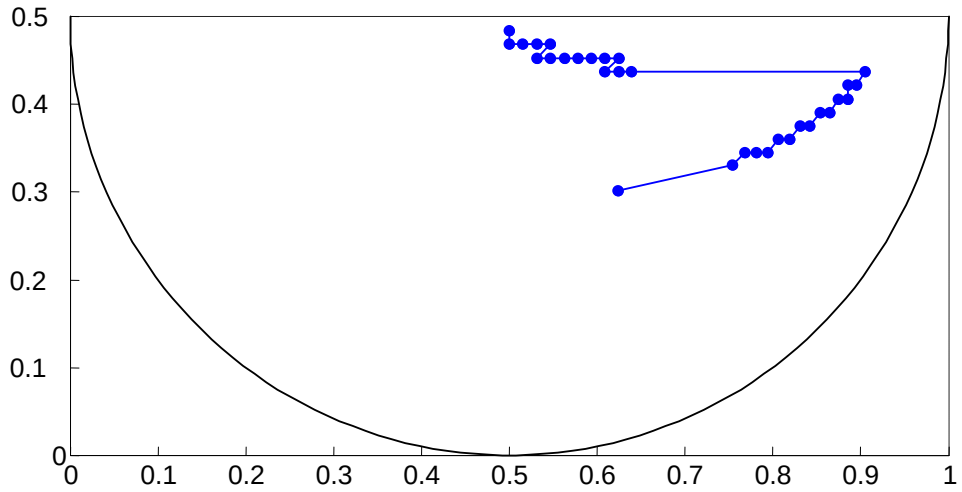

Figure 6. Transient plots of primary vortex center

CONCLUSIONS

It can be concluded that, by using a non-uniform grid, it is possible to simulate a semi-circular lid-driven cavity. The simulation achieves a steady state at 27.7 seconds. Validations are conducted for both the experiments and simulations. For the experiment, the time taken to achieve a steady state does agree with the current finding. Meanwhile for the simulation validation, the streamfunction value at the steady state differs by only 5%. In addition, the streamline pattern shows a secondary vortex appearing at the later part of the simulation, and the vorticity contour shows rapid changes at the same time. The primary vortex center also shows movement from the middle section and ends up at the middle bottom of the cavity.

ACKNOWLEDGEMENTS

The authors would like to thank the Faculty of Mechanical Engineering of Universiti Malaysia Pahang (Bumpus) and Universiti Malaysia Pahang for financial support under RDU110382.

REFERENCES

Albensoeder, S., Kuhlmann, H. C., & Rath, H. J. (2001). Multiplicity of steady two-dimensional flows in two-sided lid-driven cavities. *Theoretical and Computational Fluid Dynamics,* 14(4), 223-241.

Azwadi, C. S. N., & Idris, M. S. (2010). Finite different and lattice boltzmann modelling for simulation of natural convection in a square cavity. *International Journal of Mechanical and Materials Engineering,* 5(1), 80-86.

Barragy, E., & Carey, G. F. (1997). Stream function-vorticity driven cavity solution using p finite elements. *Computers & Fluids,* 26(5), 453-468.

Bumpus, S. R. J. (2002). *Experimental setup and testing of fiber reinforced composite structures.* (Master), University of Victoria.

Cheng, M., & Hung, K. C. (2006). Vortex structure of steady flow in a rectangular cavity. *Computers & Fluids,* 35(10), 1046-1062.

Energy Information Bureau (EIB) Malaysia.). Retrieved April 22, 2010, from http://eib.org.my/index.php?page=article&item=100,136,143,152.

Erturk, E., & Gokcol, O. (2007). Fine grid numerical solutions of triangular cavity flow. *The European Physical Journal- Applied Physics,* 38(1), 97-105.

Ghia, U., Ghia, K. N., & Shin, C. T. (1982). High-re solutions for incompressible flow using the navier-stokes equations and a multigrid method. *Journal of Computational Physics,* 48(3), 387-411.

Glowinski, R., Guidoboni, G., & Pan, T. W. (2006). Wall-driven incompressible viscous flow in a two-dimensional semi-circular cavity. *Journal of Computational Physics,* 216(1), 76-91.

Idris, M. S., Ammar, M., & M Irwan, M. A. (2012). Steady state vortex structure of lid driven flow inside shallow semi ellipse cavity. *Journal of Mechanical Engineering and Sciences (JMES),* 2, 133-147.

Kosinski, P., Kosinska, A., & Hoffmann, A. C. (2009). Simulation of solid particles behaviour in a driven cavity flow. *Powder Technology,* 191(3), 327-339.

Mercan, H., & Atalık, K. (2009). Vortex formation in lid-driven arc-shape cavity flows at high reynolds numbers. *European Journal of Mechanics - B/Fluids,* 28(1), 61-71.

Migeon, C., Texier, A., & Pineau, G. (2000). Effects of lid-driven cavity shape on the flow establishment phase. *Journal of Fluids and Structures,* 14(4), 469-488.

Patankar, S. (1980). *Numerical heat transfer and fluid flow*: CRC Press.

Veldman, A., & Rinzema, K. (1992). Playing with nonuniform grids. *Journal of engineering mathematics,* 26(1), 119-130.

Wahba, E. M. (2009). Multiplicity of states for two-sided and four-sided lid driven cavity flows. *Computers & Fluids,* 38(2), 247-253.

Yang, F., Shi, X. M., Guo, X. Y., & Sai, Q. Y. (2012). Mrt lattice boltzmann schemes for high reynolds number flow in two-dimensional lid-driven semi-circular cavity. *Energy Procedia,* 16, Part A(0), 639-644.

Zhang, T., Shi, B., & Chai, Z. H. (2010). Lattice boltzmann simulation of lid-driven flow in trapezoidal cavities. *Computers & Fluids*, 39(10), 1977-1989.

Zin, M. R. M., & Sidik, N. A. C. (2010). An accurate numerical method to predict fluid flow in a shear driven cavity. *International Review of Mechanical Engineering*, 4(6).